Multiple Piecewise Constant Active Contours for Image Segmentation using Graph Cuts Optimization

Wenbing Tao and Xue-cheng Tai

Abstract In the paper a multiple piecewise constant (MPC) active contour model is proposed to extract foreground and background of digital images. The region-based model of active contour without edges, i.e. the CV model [11] has difficulties to handle images having inhomogeneous object and background or multiple objects with different features such as color, texture or shape. Based on CV model we propose to model the interior and exterior of the evolutional curve by multiple constant intensity values instead of one constant. The constants can be obtained by clustering the interior region and the exterior region into multiple sub-regions. For better boundary capture capability, the geodesic active contour (GAC) is incorporated into the proposed MPC model to constraint the evolution of the curve. We show that the new model can be effectively solved by the graph cuts algorithms with less computational costs. Numerical experiments show that the new model can effectively segment difficult images with inhomogeneous object and background, and has superior performance compared to the original CV model. The introduction of GAC into the proposed MPC model is also demonstrated to have better boundary locating properties.

Key words: Multiple piecewise constant, active contour without edges, geodesic active contour, graph cuts, image segmentation, level set.

I. INTRODUCTION

Active contours models based on variational methods have been extensively applied to a wide range of computer vision problems including image segmentation, edge detection and visual tracking [1-4]. Active contour model can provide smooth and closed contours, which are necessary and can be readily used for further applications, such as shape analysis and recognition. Moreover, it can be easily formulated under an energy minimization framework, and allow the

incorporation of various prior knowledge, such as shape and intensity distribution, for robust image segmentation [5, 6]. The active contours method based on variational cost functionals can be roughly categorized as edge-based models [7-10] and region-based models [11-15,42,43].

Edge-based models use local image gradients information to attract the active contour toward the object boundaries. The model of Caselles et al. [7] for the geodesic active contour (GAC) is defined along a curve *C* and minimized by evolving the curve in the normal direction. Due to the local minimization, this type of edge-based approach has dependences on the initial curve. By initializing curves at different image locations, different objects of interest can be captured. This type of highly localized image information has also been found to be very sensitive to image noise.

Region-based models aim to identify each region of interest by using a certain region descriptor to guide the motion of the active contour. A well known example for the region modeling cost function is the Mumford-Shah function [16, 21]. A simplified version of the functional, which models the image with piecewise constant functions, has been studies in Chan and Vese [11] in connection with the level set idea. Recently, some variants of this model have been proposed in [42,43].These piecewise constant models are based on the assumption that image intensities are statistically homogeneous (roughly a constant) in each region. Region-based approaches have some advantages compared to edge-based methods. For example, they are robust against initial curve placement and insensitive to image noise. However, segmenting heterogeneous objects or multiple objects with different intensity distribution occur often in real applications. Techniques that attempt to model regions using non-local statistics are usually not ideal.

Lankton et al. [20] and Daralti et al. [21] propose to overcome object intensity inhomogeneity by using a localized energy that is based on the piecewise constant model of Chan and Vese [11]. The localization can improve the segmentation provided by globally defined energy in certain circumstances, but the loss of global characteristic leads to the increase of the sensitivity to the initial curve placement. The scale of localization is also hard to decide adaptively for different image objects. The segmentation of multiple objects can’t be effectively solved by such localized methods unless multiple initial curves are placed around these objects at the same time.

The problems can be partially tackled by more sophisticated models than piecewise constant models. Vese and Chan [15] propose to cast image segmentation as a problem of finding an

optimal approximation of the original image by a piecewise smooth function. Although this model has exhibits certain capability of handling intensity inhomogeneity, it is computationally expensive and often fails to give satisfactory results for real applications.

In this paper, we propose an improved region-based active contours model that can effectively overcome the problem with intensity inhomogeneity and multiple objects. We change each of the two constants that model the regions inside and outside the curve in the model of Chan and Vese (CV) [11] so that they are relevant not only to the location of the curve, but also to the intensity of the current pixel. We use multiple constant values for the regions inside and outside the curve. This multiple piecewise constant (MPC) model can segment objects with intensity inhomogeneity and multiple objects. In the CV model [11], the boundary of the curve is constrained by the length, which doesn't consider the gradient information of the boundary. In [40], Bresson et.al. propose to unify CV model and GAC model and state the existence of the global minimization of this energy function. We also integrate the edge-based model such as geodesic active contour into the proposed MPC model for better boundary capture capability. Furthermore, we will show that the proposed active contour model can be effectively solved using the graph cut algorithm [17, 18, 19,39] for much higher computational efficiency than the usually used level set framework [41, 42].

The minimal cut problem is to find a cut whose capacity is the minimum over all cuts of the graph **G**. Due to max-flow min-cut theorem by Ford and Fulkerson [28], there are several fast algorithms to solve the minimal cut problem of graph **G** by solving the corresponding maximal flow problem. See [18] for a detailed discussion about the implementation and comparison of several algorithms. The graph cuts method was first introduced into computer vision as an optimizing tool by Greig et. al. [29] in connection with markov random fields. It has later been studied by Boykov and Kolmogorov [18, 27, 31]. By optimizing the energy function based on the maximization of the posteriori probability (MAP) and markov random fields (MRF), some interactive image segmentation methods based on graph cuts [19, 38, 30] have been proposed. Recently, graph cuts method has also received a lot of attention due to its connection with continuous variational problem and PDEs [26, 32-35, 39, 41, 42].

The outline of the paper is as follows. In the next section we introduce our model as an energy minimization problem and discuss the relationship with the other existing models. We formulate

the model in terms of level set functions. In section III we show that the proposed energy functional can be converted into the graph cuts framework and be effectively minimized by means of graph cuts algorithms. An iterative segmentation procedure that alternates between estimation and parameter learning is presented. In section IV we validate our model and algorithm by numerical results on synthetic images and real natural images, showing the advantages of our proposed model and segmentation algorithm, followed by a brief conclusion section.

II. REGION-BASED ACTIVE CONTOUR MODEL

Let $\Omega \subset \Re^2$ be the image domain, and $u_0 : \Omega \to \Re$ be a given gray image. Let *C* be a closed subset in Ω, made up of a finite set of smooth curves. The connected components of $\Omega \setminus C$ are denoted by Ω_i, such that $\Omega = \cup \Omega_i \cup C$. We also denote by $|C|$ the length of a curves *C*. Let $u : \Omega \to \Re$ be a given bounded image-function. The image segmentation problem can be formulated as finding the minimizer of the following cost functional [22]:

$$F^{MS}(u, C) = \int_{\Omega} (u_0 - u)^2 dx + \mu \int_{\Omega \setminus C} |\nabla u|^2 dx + \nu |C|, \tag{1}$$

where μ and ν >0 are fixed parameters, to weight the different terms in the energy. The minimization of Mumford-Shah functional results in an optimal contour *C* that segments the given image u_0, and *u* is an optimal piecewise smooth approximation of the given image u_0, and is smooth within each of the connected components in the image domain Ω separated by the contour *C*.

For many applications, it is enough to assume that *u* is a piecewise constant function, i.e., *u*=constant c_i inside each connected component Ω_i, and the problem is often called the "minimal partition problem". For such case, the second term disappears from the above minimization functionals. One reduced model of (1), active contour without edge, i.e., CV model, is proposed by Chan and Vese [11] as follows.

$$F^{CV}(c_1, c_2, C) = \lambda_1 \iint_{\Omega_1} (u_0(x, y) - c_1)^2 + \lambda_2 \iint_{\Omega_2} (u_0(x, y) - c_2)^2 + \nu \oint ds, \tag{2}$$

where Ω_1 corresponds to the interior and Ω_2 corresponds to the exterior of the curve *C*, constants c_1 and c_2 depending on *C*, approximate the image intensity of Ω_1 and Ω_2, are usually

the averages of $u_0(x, y)$ in Ω_1 and Ω_2 respectively. Among the ways of representing the unknown interfaces, the level set method is the most elegant due to its ability in dealing with unknown topology. In [11], the curve is represented by a level set formulation, and the energy minimization problem is converted to solving a level set evolution equation [11]. The main drawback of level set method is expensive computation.

Let $u_0(x, y)$ denote the input image defined on the domain Ω, and let C be a closed contour represented as the zero level set of a signed distance function ϕ, i.e., $C = \{x \mid \phi(x) = 0\}$, c.f. [23, 24]. We specify the interior of C by the following approximation of the smoothed Heaviside function $H(\phi(x, y))$ and the exterior of C is defined as $1 - H(\phi(x, y))$. To specify the area just around the curve, we will use the derivative of $H(\phi(x, y))$, a smoothed version of the Dirac delta [25]. A level set formulation that represents the approximated piecewise constant function is as follows.

$$u(x, y) = c_1 H(\phi(x, y)) + c_2(1 - H(\phi(x, y))), (x, y) \in \Omega, \tag{3}$$

where the discontinuity sets (the active contours) lie on the interface $\{C(x, y) \mid \phi(x, y) = 0\}$, and the length of the interface is represented as $\int_\Omega |\nabla H(\phi)|$. Then the energy function of active contours without edges model is formulated as follows.

$$\begin{aligned} F^{CV}(c_1, c_2, \phi) = {} & \lambda_1 \int_\Omega (u_0(x, y) - c_1)^2 H(\phi) dxdy \\ & + \lambda_2 \int_\Omega (u_0(x, y) - c_2)^2 (1 - H(\phi)) dxdy + \nu \int_\Omega |\nabla H(\phi)| dxdy \end{aligned}. \tag{4}$$

Keeping ϕ fixed and minimizing the energy $F^{CV}(c_1, c_2, \phi)$ with respect to the constants c_1 and c_2, it is easy to express these constants as a function of ϕ by

$$c_1(\phi) = \frac{\int_\Omega u_0(x, y) H(\phi(x, y)) dxdy}{\int_\Omega H(\phi(x, y)) dxdy}, \tag{5}$$

$$c_2(\phi) = \frac{\int_\Omega u_0(x, y)(1 - H(\phi(x, y))) dxdy}{\int_\Omega (1 - H(\phi(x, y))) dxdy}. \tag{6}$$

Keeping c_1 and c_2 fixed, and minimizing the energy $F^{CV}(c_1, c_2, \phi)$ with respect to ϕ, we

deduce the associate Euler-Lagrange equation for ϕ. Parameterizing the descent direction by an artificial time $t \geq 0$, the equation in $\phi(t,x,y)$ (with $\phi(0,x,y) = \phi_0(x,y)$ defining the initial contour) is as follows.

$$\frac{\partial \phi}{\partial t} = \delta(\phi)[\nu(div(\frac{\nabla \phi}{|\nabla \phi|}) - \lambda_1(u_0(x,y) - c_1)^2 + \lambda_2(u_0(x,y) - c_2)^2]. \quad (7)$$

For numerical simulations, the functions $H(\phi)$ and $\delta(\phi)$ are replaced by some smoothed regularizations. $\delta(\phi)$ is usually replaced with $|\nabla \phi|$. The gradient decent equation is solved using an explicit finite difference scheme. Note that this algorithm only evolves the interface in a local sense. Chan et al. [11] also proposed a heuristic method to define the Heaviside function as well as its derivative. It takes account of global information. However, such compromise may lead the result to deviate from the right solution, since the numerical approximation of Heaviside function is very loose.

III. DESCRIPTION OF PROPOSED MODEL AND LEVEL SET FORMULATION

We now introduce an improved version of region-based modeling by Chan et al, i.e., multiple piecewise constant (MPC) active contours model. The basic form of the cost functional is as following:

$$\begin{aligned} F^{MPC}(c_1, c_2, C) = \lambda_1 \iint_{\Omega_1} (u_0(x,y) - c_1(x,y))^2 \\ + \lambda_2 \iint_{\Omega_2} (u_0(x,y) - c_2(x,y))^2 + \nu \oint ds \end{aligned}, \quad (8)$$

where $c_1(x,y)$ and $c_2(x,y)$ are piecewise constant function that models the image regions inside *C* and outside *C*. We next show how to decide the piecewise constant functional $c_1(x,y)$ and $c_2(x,y)$.

We first cluster the region Ω_1 into n_1 sub-regions $\{\Omega_{1k}, k = 1, \cdots, n_1\}$ by *k*-means method and give the sub-region Ω_{1k} the label $k, (k = 1, \cdots, n_1)$. Then we can get the label functional of region Ω_1 as follows:

$$\pi_1(x,y) = k, if\,(x,y) \in \Omega_{1k}, \quad (9)$$

where $k = 1, \cdots, n_1$ and n_1 is the clustering number of region Ω_1.

Similarly, we can get the label functional of region Ω_2 as

$$\pi_2(x, y) = k, if\ (x, y) \in \Omega_{2k}, \tag{10}$$

where $k = 1, \cdots, n_2$ and n_2 is the clustering number of region Ω_2.

Similar as in [42, 43], we define the following function

$$\psi(x) = \begin{cases} 1, & x = 0 \\ 0, & otherwise \end{cases}. \tag{11}$$

Then we can compute $c_1(k)$ and $c_2(k)$ according to the following equations:

$$c_1(k) = \frac{\int_{\Omega_1} u_0(x, y)\psi(\pi_1(x, y) - k)dxdy}{\int_{\Omega_1} \psi(\pi_1(x, y) - k)dxdy}, \tag{12}$$

$$c_2(k) = \frac{\int_{\Omega_2} u_0(x, y)\psi(\pi_2(x, y) - k)dxdy}{\int_{\Omega_2} \psi(\pi_2(x, y) - k)dxdy}. \tag{13}$$

Once the values of $c_1(k)$ and $c_2(k)$ have been determined, the MPC model can be represented as:

$$\begin{aligned} F^{MPC}(c_1, c_2, C) = \lambda_1 \iint_{\Omega_1} \underset{k=1\cdots n_1}{Min} (u_0(x, y) - c_1(k))^2 \\ + \lambda_2 \iint_{\Omega_2} \underset{k=1\cdots n_2}{Min} (u_0(x, y) - c_2(k))^2 + \gamma \oint ds \end{aligned}. \tag{14}$$

Notice that the third term of multiple piecewise constant (MPC) active contours model is the length of the curve *C*, which can be replaced by the geodesic active contour (GAC) proposed by Caselles et al. [7] for better boundary capture capability. Then we get the combination of region-based and edge-based models:

$$\begin{aligned} F^{MPC}(c_1, c_2, C) = \lambda_1 \iint_{\Omega_1} \underset{k=1\cdots n_1}{Min} (u_0(x, y) - c_1(k))^2 \\ + \lambda_2 \iint_{\Omega_2} \underset{k=1\cdots n_2}{Min} (u_0(x, y) - c_2(k))^2 + \nu \oint g(C)ds \end{aligned}, \tag{15}$$

where $g = 1/(1 + \beta|\nabla u_0|)$.

The above mode integrates the advantages of the region-based modes, i.e., robustness to initialization and insensitivity to image noise, and the advantages of the edge-based models, i.e.,

good local characteristic and boundary capture capability. We can use level set method to solve this problem and the corresponding level set energy functional is:

$$\begin{aligned} F^{MPC}(c_1, c_2, \phi) = \lambda_1 \int_\Omega \underset{k=1\cdots n_1}{Min} (u_0(x,y) - c_1(k))^2 H(\phi) dxdy \\ + \lambda_2 \int_\Omega \underset{k=1\cdots n_2}{Min} (u_0(x,y) - c_2(k))^2 (1 - H(\phi)) dxdy \\ + \nu \int_\Omega |\nabla H(\phi)| g(x,y) dxdy \end{aligned} . \quad (16)$$

The gradient descent equation is

$$\begin{aligned} \frac{\partial \phi}{\partial t} = \delta(\phi)[\nu(div(g(x,y)\frac{\nabla \phi}{|\nabla \phi|}) \\ - \lambda_1 \underset{k=1\cdots n_1}{Min} (u_0(x,y) - c_1(k))^2 + \lambda_2 \underset{k=1\cdots n_2}{Min} (u_0(x,y) - c_2(k))^2] \end{aligned} . \quad (17)$$

Since we model region inside *C* and outside *C* by using two multiple piecewise constant functions $c_1(k)$ and $c_2(k)$, not two constants c_1 and c_2, the parameters can't be updated using formula (5) and (6). The parameters $\{c_1(k), k = 1, \cdots, n_1\}$ and $\{c_2(k), k = 1, \cdots, n_2\}$ can be updated iteratively with the interface evolution, i.e.

$$c_1(k, \phi) = \frac{\int_\Omega u_0(x,y) H(\phi(x,y)) \psi(\pi_1(x,y) - k) dxdy}{\int_\Omega H(\phi(x,y)) \psi(\pi_1(x,y) - k) dxdy}, k = 1, \cdots, n_1, \quad (18)$$

$$c_2(k, \phi) = \frac{\int_\Omega u_0(x,y)(1 - H(\phi(x,y))) \psi(\pi_2(x,y) - k) dxdy}{\int_\Omega (1 - H(\phi(x,y))) \psi(\pi_2(x,y) - k) dxdy}, k = 1, \cdots, n_2. \quad (19)$$

It is time consuming to solve the gradient decent problems using numerical methods. In the next section, we shall develop some efficient methods by transforming the problem into a graph cut problem.

IV. GRAPH CUTS OPTIMIZATION FOR MPC MODEL

In section III, we have described the proposed MPC active contour model integrated with GAC and the level set formulation. In this section, we will show that our proposed model can be effectively optimized by graph cut algorithms. Thanks to the fast global minimization of graph cuts algorithm, the speed and the accuracy of the implementation are greatly improved, and make the result much less sensitive to initialization since the optimization is more global.

Given a graph **G**=(**V**, **E**, **W**), where V is the set of vertices, **E** is the set of edges, and **W** is the set of nonnegative weights on the edges. There are two specially designated terminal nodes *s*(source)

and *t*(sink) in the graph. For every node *v* in **G**, there is a path from source *s* to sink *t* via *v*. This kind of graphs are called flow network. For this kind of graph, the edges that are out of source *s* and the edges that are into sink *t* are called *t*-link. The edges that connect the other nodes except for *s* and *t* are called *n*-link. A cut on G is a partition of the vertices **V** into two disjoint sets **S** and **T** such that $s \in S$ and $t \in T$. For a given cut(**S**, **T**), the cost of the cut is defined as

$$\left|C\right|_G = \sum_{p \in S, q \in T} \omega_{pq}, \tag{20}$$

where ω_{pq} is the weight of edge connecting node *p* and *q*.

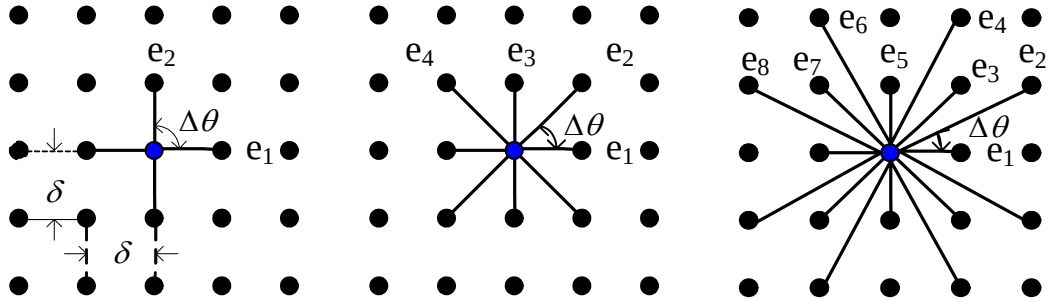

Fig. 1 Left: N_4 neighbor system; middle: N_8 neighbor system; right: N_{16} neighbor system

In [26], Boykov and Kolmogrov introduced a notation of *cut metric* on graphs. Consider a cut on a grid-graph **G** as a closed contours (in R^2). Length can be defined for a cut. By Cauchy-Crofton formula, the connection between Euclidean length $\left|C\right|_E$ of a curve *C* in R^2 and a measure of a set of lines intersecting it can be established. Then by some reasonably partitioning, the following discrete formula can be used to approximate the length of the contours.

$$\left|C\right|_E = \sum_{d=1}^{n_G} (n_c(d) \cdot \frac{\delta^2 \cdot \Delta\theta}{2 \cdot \left|e_d\right|}), \tag{21}$$

where $n_c(d)$ is the total number of intersections of *C* with the edge lines in the d^{th} direction vector, i.e., e_d, see Fig. 1 for e_d, δ and $\Delta\theta$. If we choose constant edge weights within each family of edge lines as

$$\omega_d = \frac{\delta^2 \cdot \Delta\theta}{2 \cdot \left|e_d\right|}, \tag{22}$$

then we have

$$\left|C\right|_E = \sum_{d=1}^{n_G} n_c(d)\cdot\omega_d \approx \left|C\right|_G . \tag{23}$$

A. Discrete Representation of Energy Functional

The equations (15) or (16) are continuous energy functional in $\Omega \subset \Re^2$. We must discretize them to take values on a grid so that they can be applied in image domain. Let $P = \{(i,j) \mid i \in \{1,\cdots,n\}, j \in \{1,\cdots,m\}\}$ be the set of image grid points, the mesh size is one, and $N = mn$ is the number of the grid points in *P*. Consider all the pixels $u(i,j)$ of the image domain P, we define a binary grid function $\{x_{ij} \mid x_{ij} \in \{0,1\}, (i,j) \in P\}$ to represent a partition as in [43]. For simpler expression, let $p = (i,j) \in P$. We define x_p as

$$x_p = \begin{cases} 1, & \text{if } \phi_p \geq 0 \\ 0 & \text{otherwise} \end{cases} . \tag{24}$$

Therefore, the first two terms in the energy functional (15) can be discretized as

$$E_1 + E_2 = \lambda_1 \sum_{p\in P} \underset{k=1\cdots n_1}{Min} (u_0(p) - c_1(k))^2 x_p + \lambda_2 \sum_{p\in P} \underset{k=1\cdots n_2}{Min} (u_0(p) - c_2(k))^2 (1-x_p) . \tag{25}$$

From (22), the discrete form of the length of the curve $\oint ds$ can be expressed as follows

$$\left|C\right|_E = \left|C\right|_G = \sum_{p\in P} \sum_{q\in N_r(p)} \omega_{pq}((1-x_p)x_q + x_p(1-x_q)), \tag{26}$$

where $\omega_{pq} = \omega_d$ if $(p,q) \in e_d$, $d = 1,\cdots,n_G$ and $N_r(p)$ is the neighbor system of *p* defined in Fig. 1 and *r*=4, 8 or 16.

The third term of (15) is the geodesic active contour $\nu \oint g(C)ds$ where $g = 1/(1+\beta|\nabla u_0|)$, i.e., the integral of $dg = 1/(1+\beta|u_0(p) - u_0(q)|), q \in N_r(p)$ along the curve C. Using similar argument as getting (26), the discrete form of the third term of (15), $\nu \oint g(C)ds$, can be expressed as follows

$$E_3 = \nu \sum_{p\in P} \sum_{q\in N_r(p)} \frac{\omega_{pq}((1-x_p)x_q + x_p(1-x_q))}{1+\beta|u_0(p) - u_0(q)|} . \tag{27}$$

Therefore, the discrete formation of equation (15) is as follows

$$E^{MPC}(c_1,c_2,x)=\lambda_1\sum_{p\in P}\underset{k=1\cdots n_1}{Min}(u_0(p)-c_1(k))^2x_p+\lambda_2\sum_{p\in P}\underset{k=1\cdots n_2}{Min}(u_0(p)-c_2(k))^2(1-x_p)+\nu\sum_{p\in P}\sum_{q\in N_r(p)}\frac{\omega_{pq}((1-x_p)x_q+x_p(1-x_q))}{1+\beta\left|u_0(p)-u_0(q)\right|} \quad . \tag{28}$$

B. Energy Minimization using Graph Cuts Framework

Equation (28) is a typical energy functional that can be optimized by graph cuts method [27]. Construct a flow network graph **G**=(**V**, **E**, **W**) with one source node *s* and sink node *t*. Each pixel in image domain is considered as one node of **G**. Each pixel node *p* has two *t*-link {*s*, *p*} and {*p*, *t*} respectively connecting it to the source and sink nodes and the weights are respectively defined as w_{sp} and w_{pt}. Each pair neighboring pixels {*p*, *q*} in neighbor system is connected by an *n*-link and the weight is defined as w_{pq}. The weights of **G** are set according to the following equations:

$$w_{sp}=\lambda_1\underset{k=1\cdots n_1}{Min}(u_0(p)-c_1(k)),\ p\in P,k=1,\cdots,n_1, \tag{29}$$

$$w_{pt}=\lambda_2\underset{k=1\cdots n_2}{Min}(u_0(p)-c_2(k)),\ p\in P,k=1,\cdots,n_2, \tag{30}$$

$$w_{pq}=\frac{\nu\omega_{pq}}{1+\beta\left|u_0(p)-u_0(q)\right|},\ p\in P,\ \forall q\in N_r(p). \tag{31}$$

After setting the weights of the edges of **G**, the minimum cut of **G** can be computed by the typical max-flow min-cut algorithm such as augmenting path style method [18, 36] or push-relabel style method [37]. The minimum cut corresponds to the minimum energy value of functional $E^{MPC}(c_1,c_2,x)$ of (28). We can also get a group binary label $\{x_p\mid x_p\in\{0,1\},p=1,\cdots,N\}$. Let $P_1=\{p\mid x_p=1,p=1,\cdots,N\}$ and $P_2=\{p\mid x_p=0,p=0,\cdots,N\}$. We respectively cluster P_1 and P_2 into n_1 and n_2 subsets and get the label functional $\pi_1(p)$ and $\pi_2(p)$ that are defined in formula (9) and (10). Then the optimal estimation of the parameters $\{c_1(k),k=1,\cdots,n_1\}$ and $\{c_2(k),k=1,\cdots,n_2\}$ are obtained using the following two equations:

$$c_1(k,x)=\frac{\sum_{p\in P}u_0(p)x_p\psi(\pi_1(p)-k)}{\sum_{p\in P}x_p\psi(\pi_1(p)-k)},k=1,\cdots,n_1, \tag{32}$$

$$c_2(k,x)=\frac{\sum_{p\in P} u_0(p)(1-x_p)\psi(\pi_2(p)-k)}{\sum_{p\in P}(1-x_p)\psi(\pi_2(p)-k)}, k=1,\cdots,n_2, \tag{33}$$

where $\psi(x)$ is defined in formula (11).

The multiple piecewise constant approximation of *u* is

$$u(p)=\begin{matrix}\sum_{k=1}^{n_1} c_1(k)x_p\psi(\pi_1(p)-k)\\ +\sum_{k=1}^{n_2} c_2(k)(1-x_p)\psi(\pi_2(p)-k)\end{matrix}, \quad p\in P. \tag{34}$$

Then we can construct an iterative algorithm that alternates between estimation and parameter learning to get the optimal multiple piecewise constant approximation of *u*. To summarize, the algorithm can be described as follows.

1. Initialize the curve *C* and get the interior of *C*, i.e., Ω_1, and the exterior of *C*, i.e., Ω_2. Let the label x_p of Ω_1 is 1 and the label x_p of Ω_2 is 0.
2. Cluster the pixels with label 1 into n_1 subsets and get $\pi_1(p)$. Cluster the pixels with label 0 into n_2 subsets and get $\pi_2(p)$.
3. Estimate $\{c_1(k), k=1,\cdots,n_1\}$ and $\{c_2(k), k=1,\cdots,n_2\}$ according to (32) and (33).
4. Construct graph **G** by (29)-(31), compute the minimum cut of **G** using graph cuts algorithm and get the binary label $\{x_p \mid x_p\in\{0,1\}, p=1,\cdots,N\}$ of the image.
5. Repeat from step 2, until converge.

V. EXPERIMENTS

In this section, we validate our proposed MPC model and its graph cuts optimization implementation by numerical experiments on synthetic images and real natural images. The results are compared with the original CV model [11]. We also demonstrate that our MPC model will lead to better segmentations when combined with GAC model. In MPC model, there are several parameters, λ_1, λ_2, ν and n_1 and n_2 that need to be decided. We set $\lambda_1=\lambda_2=1$. The varying parameters are ν, n_1 and n_2,. They will be set according to the different experimental

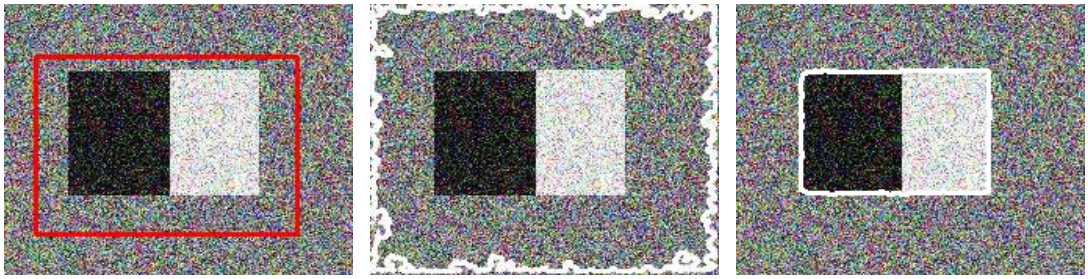

Fig. 2 The comparison of MPC model and CV model using synthetic image. Left: the image and the initial curve; middle: the result by CV model; right: the result by MPC model with n_1=n_2=2. Both models aren't integrated with GAC.

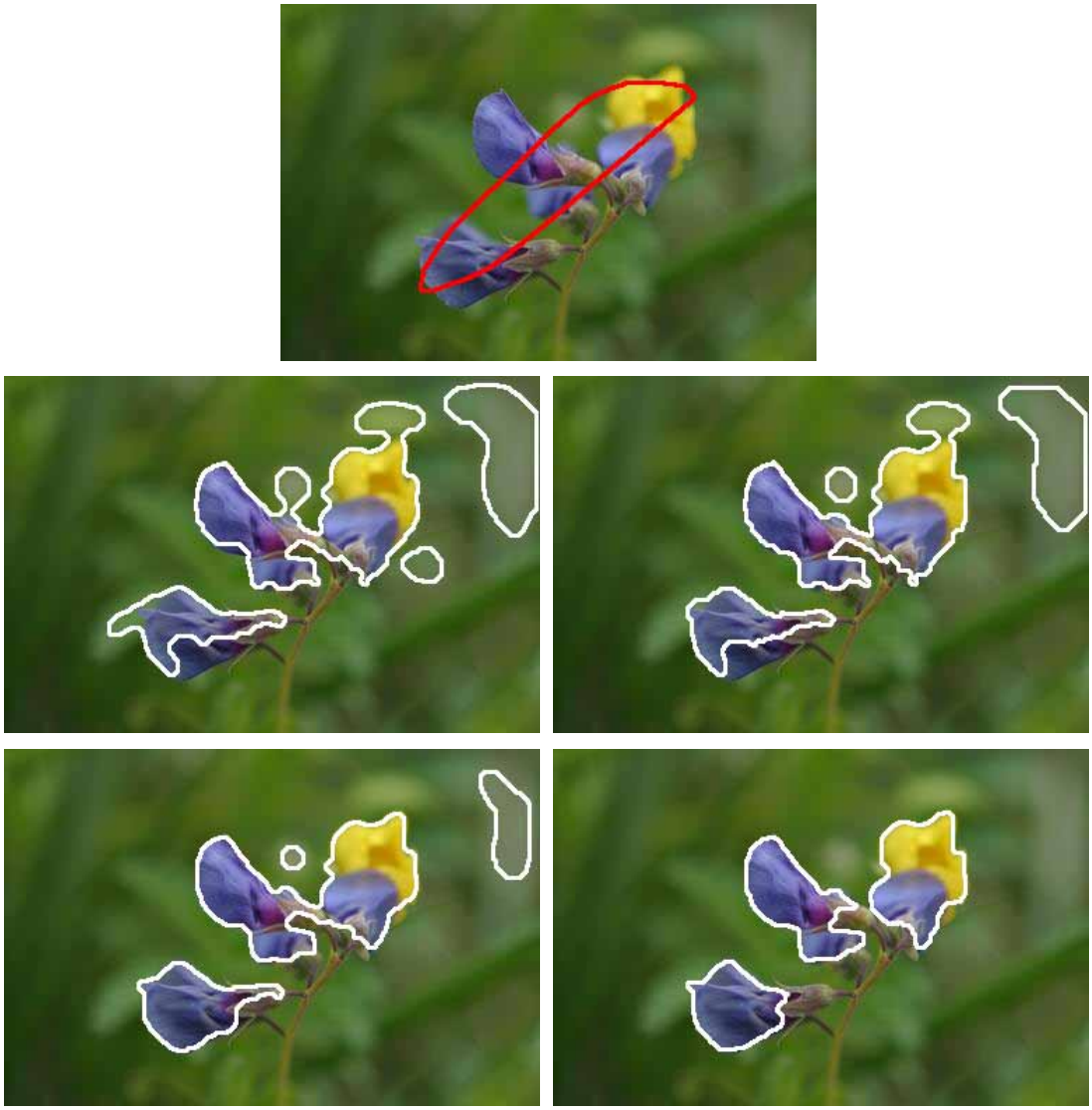

Fig. 3 Row 1 is the original flower image and the initial contour. Rows 2 are the results by MPC model without GAC, rows 3 are the results by MPC model with GAC. Columns (from left to right) are respectively the results with n_1=n_2=1, n_1=n_2=5. Parameter ν =6000 for MPC without GAC and ν =12000 for MPC with GAC.

aims so that the performance of the proposed method and the effect of the parameters can be effectively analyzed. Notice that CV model [11] is the special case of our MPC model with

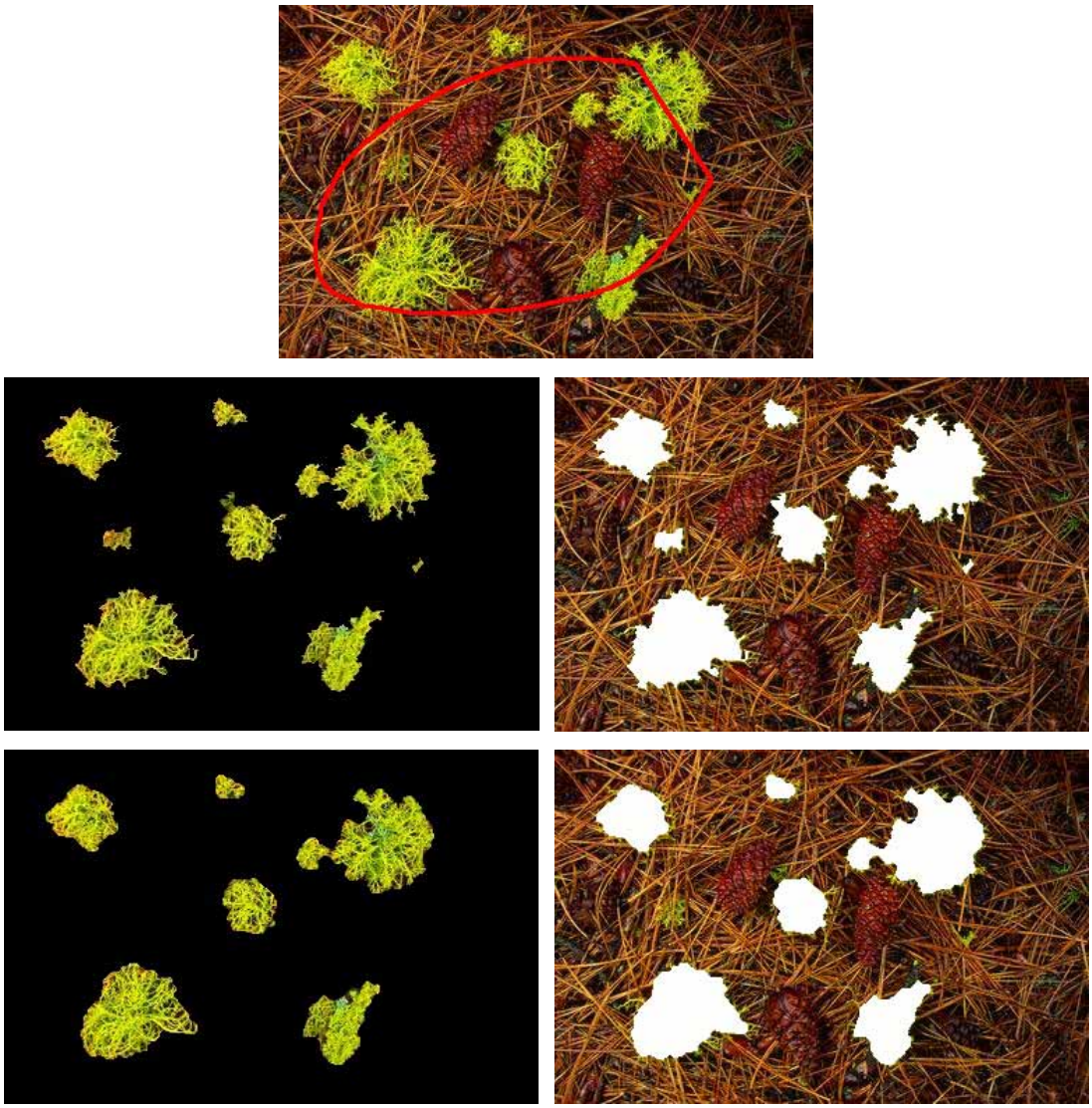

Fig. 4 Row 1: the original image and the initial contour; Row 2: the result by MPC model with GAC, foreground (left) and background (right); Row 3: the result by MPC model without GAC, foreground (left) and background (right). Parameter ν =6000 for MPC without GAC and ν =12000 for MPC with GAC, n_1=n_2=5.

n_1=n_2=1 without GAC. We give the CPU time in seconds performed on a laptop which is equipped with a 2.0-GHz Pentium CPU and 2GB memory. In our numerical algorithm, we first initialize the curve, then cluster the regions inside the curve and outside the curve into n_1 and n_2 subsets and compute $c_1(k), k = 1, \cdots, n_1$ and $c_2(k), k = 1, \cdots, n_2$, and we construct the graph and solve the min-cut problem. Then we iterate these last two steps.

Fig. 5: The test results of the horse image by MPC model with and without GAC. Row 1 and 2 are the results by MPC model without GAC. Row 3 and 4 are the results by MPC model with GAC. Row 1 and 3 (from left to right): the original image and the initial contour, the result with $n_1=n_2=1$, and $n_1=n_2=2$. Row 2 and 4 (from left to right): the results with $n_1=n_2=3$, $n_1=n_2=4$, $n_1=n_2=5$.

We first compare our MPC model with CV model using a synthetic image. The superiority of CV model combined with GAC model has been demonstrated in Fig. 8 of [40] and we will further testify that using real images in the following experiments. The original image in Fig. 2 has a rectangle object including a half black part and a half white part. Exploiting the CV model and just modeling the rectangle object and the background with only one constant will lead to the wrong segmentation result (see the middle of Fig. 2). But if we model the rectangle object and the background with two constants ($n_1= n_2=2$), the heterogeneous rectangle object can be segmented (see the right of Fig. 2). Both models in this experiment aren't integrated with GAC.

In Fig. 3 the experimental results of a real flower image are shown. The comparison between the proposed MPC model and CV model is conducted. Results with or without GAC are also given. In

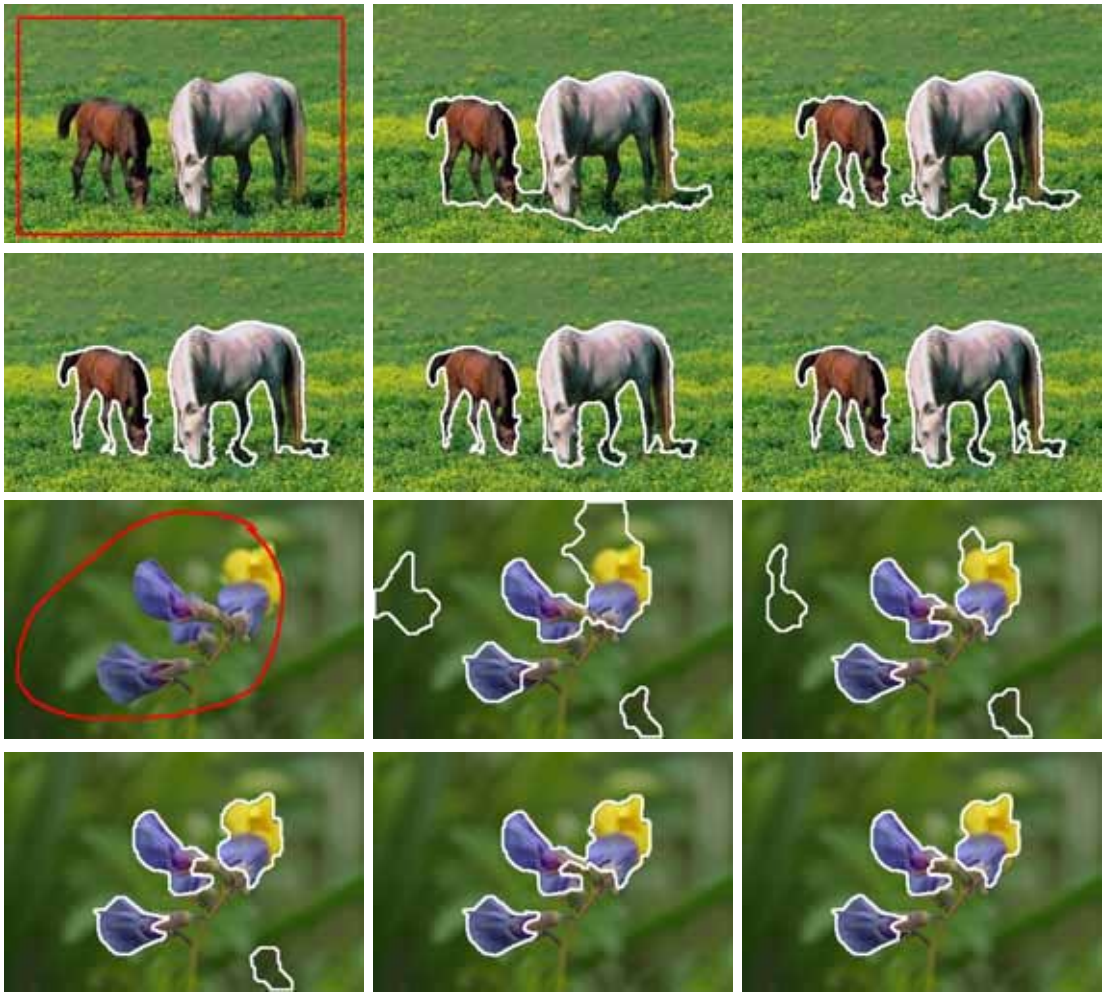

Fig. 6: The iterative process with initial contour for horse image (row 1 and 2) and flower image (row 3 and 4). Parameter n_1=n_2=5.

the MPC model, the clustering number are taken as n_1=n_2=5. The test image includes blue and yellow flowers. By use of the traditional CV model it is hard to distinguish both the blue and yellow flowers from the background. A little better result can be obtained when GAC is merged to CV model, but the intact object still can't be extracted. MPC model with n_1=n_2=5 can get better results than CV model, but when without GAC still some background information is labeled as the object. MPC model integrated with GAC leads to best performance and the blue and yellow flowers can be exactly distinguished from the background.

Fig. 4 shows the results of a brushwood image. We further demonstrate the superiority of MPC model when integrated with GAC. We can see that the curve is smoother for the model without GAC, but much detail information is lost and some small objects are undetected. Comparatively, the model with GAC can obtain more accurate segmentation and detection of the boundary of the objects.

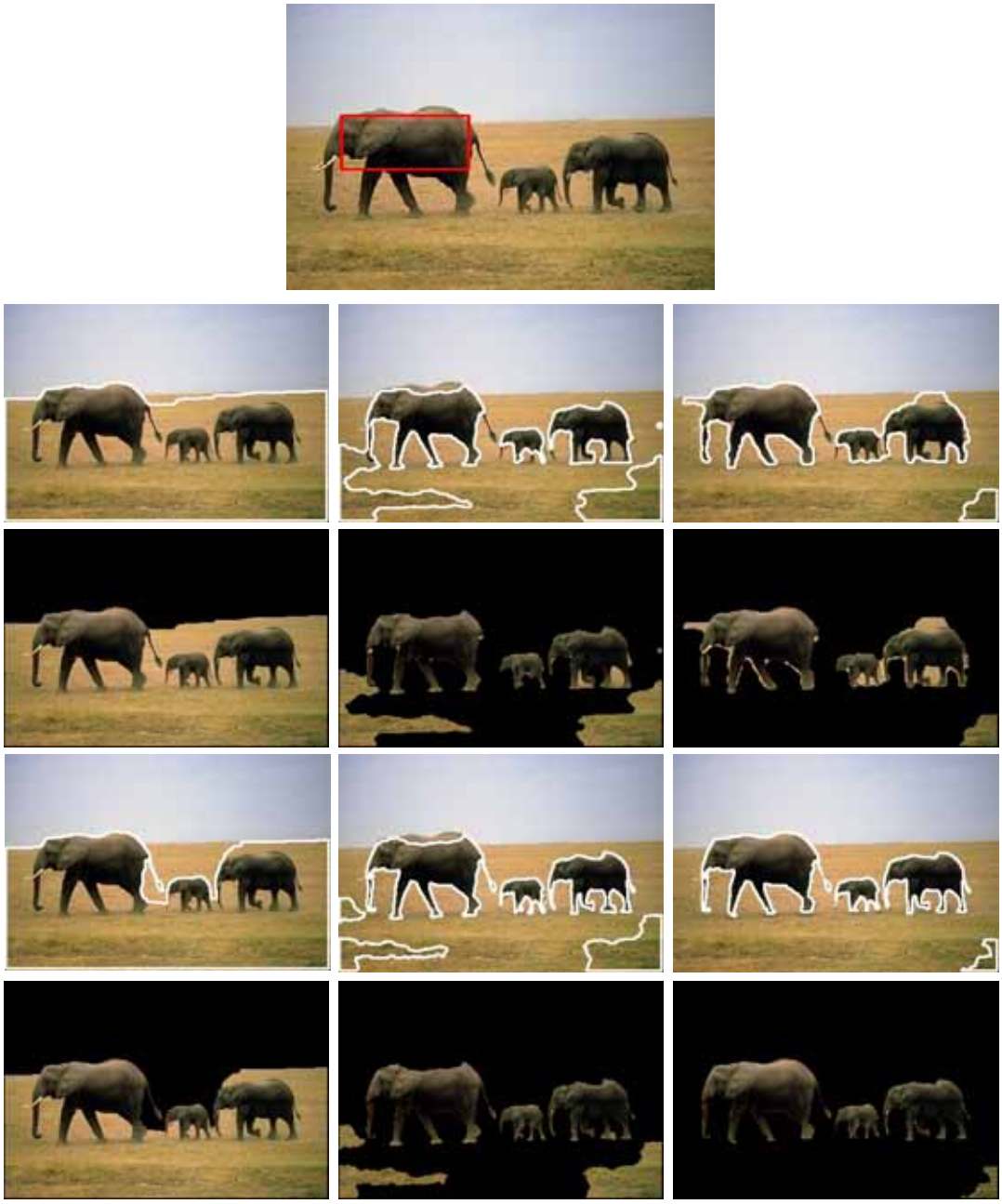

Fig. 7 Row 1 is the original elephant image and the initial contour. Rows 2 and 3 are the results by MPC model without GAC, rows 4 and 5 are the results by MPC model with GAC. Columns (from left to right) are respectively the results with $n_1=n_2=1$, $n_1=n_2=2$, $n_1=n_2=5$. Row 2 and 4 are the original images and the result contours, row 3 and 5 are the extracted foreground. Parameter ν =6000 for MPC without GAC and ν =12000 for MPC with GAC.

The experimental results of the "Horse" image are shown in Fig. 5. This image includes two horses which have different color distribution. Therefore modeling the two horses with only one constant like CV model will undoubtedly lead to inaccurate segmentation, which is shown in row 1 of Fig. 5. In the experiments of Fig. 5, different clustering number is chosen to test the

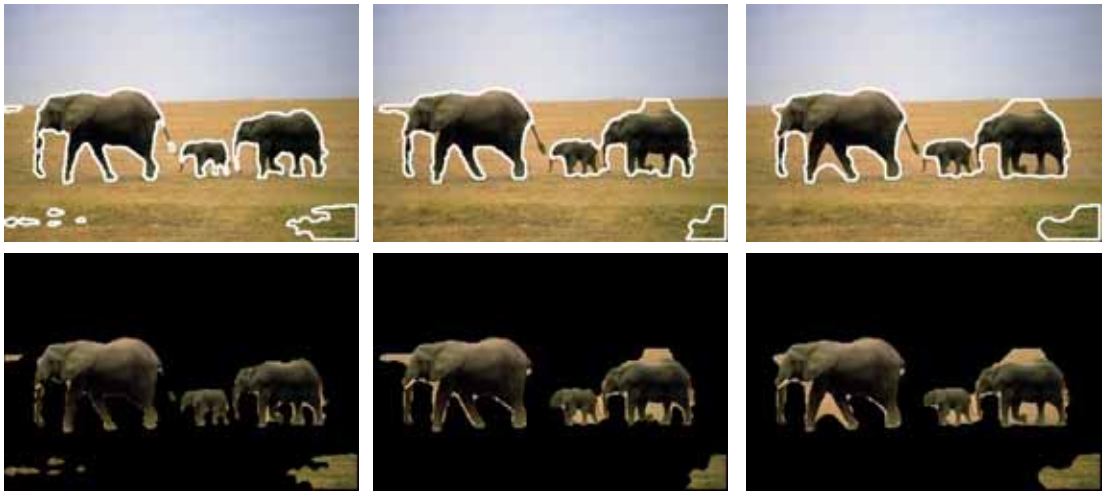

Fig. 8: The results by MPC model without GAC, n_1=n_2=5. From column 1 to 3: the parameter ν is respectively 3000, 6000, 9000. Top: the original image and the contour. Bottom: the extracted foreground.

segmentation performance of MPC model with or without GAC. We can see that the result becomes better and better as the clustering number increases from 1 to 5. When the values are larger than 5, there is no obvious improvement of the quality. Generally, the clustering number can be upto 20 according to the degree of the inhomogeneity of the objects or the number of the detected objects. From the results we can also see that better performance is obtained when the proposed model is integrated with GAC than without GAC.

In Fig. 6 the evolution of the curve for the flower and horse images are shown. Despite that the initial curves are far away, the two kinds of flowers in the flower image and the two horses with different color distribution can all be segmented satisfactorily from the background.

In Fig. 7 and 8 one elephant image is used to test our model. This image scene includes three elephant objects, the sky and the grassland background. The segmenting task is to extract three elephants from the background. In Fig. 7, we test three cases where the clustering numbers are respectively set to n_1=n_2=1, n_1=n_2=2, n_1=n_2=5. In each case we compare the results with or without GAC. From the results we see that larger clustering number leads to better results. However, if we do not include GAC, two unexpected situations appear: 1) the details of the elephant such as the legs and tails are easily lost; or 2) some background information is labeled as the foreground by mistake, for example, the background near to the legs of the elephant isn't separated out. MPC model with n_1=n_2=5 integrated with GAC can segment the elephants with perfect details.

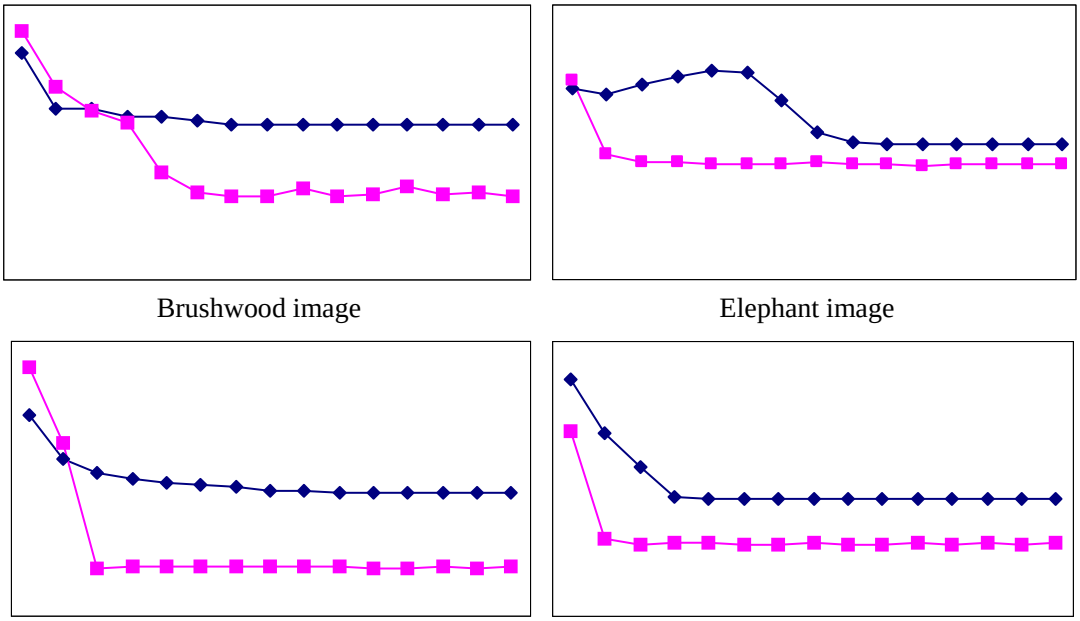

Brushwood image　　Elephant image

Flower image　　Horse image

Fig. 9: The plot of energy value of the iterative process, the iterative time is 15. The blue curve in each plot is for CV model with GAC; the red curve in each plot is for MPC model with GAC, n_1=n_2=5.

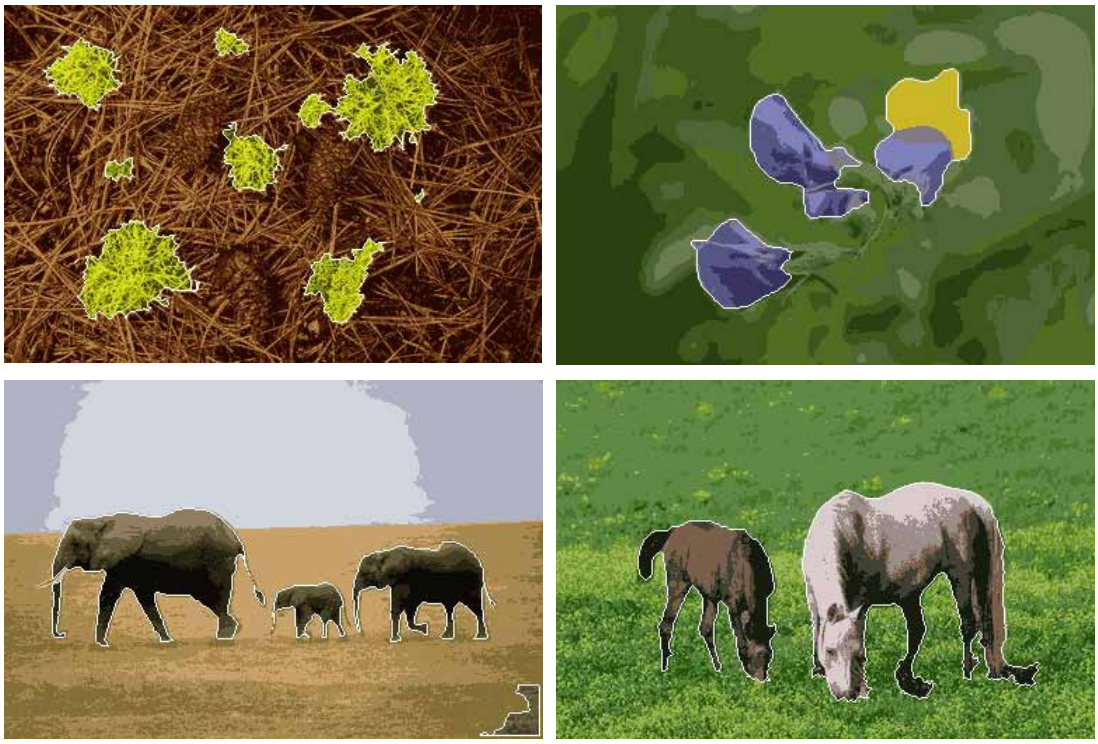

Fig. 10: The multiple piecewise constant approximation of four images after convergence by formula (34), n_1=n_2=5.

In Fig. 8 we test the effect of different parameter ν without GAC. Three different values of parameter, ν=3000, 6000 and 9000 are selected. We find when ν is set to 3000 more object

details can be extracted from the background such as the legs and tails of the elephants. But simultaneously more unexpected background information such as some noise is labeled by mistake. When larger ν is chosen, the strong constraint of the curve length which desires shorter length of the curve avoids the curve to evolve to concave boundaries such as the region between the legs of the elephants. Therefore, without GAC, just relying on the adjustment of the parameter ν we may not obtain the same satisfactory segmentation results as MPC model with GAC does.

The values of the minimization functional versus iteration number for four images are shown in Fig. 9. We compare the energy value of CV model and our MPC model with n_1=n_2=5 when the algorithms are convergent. Both models are incorporated with GAC. We can see that the energy decreases gradually as the curve evolves and MPC model has lower energy value than CV model. Fig. 10 shows the resulted images of the MPC with GAC approximation for four test images by formula (34) after convergence. The clustering number n_1=n_2=5 is chosen.

The size of the test images used in this paper is all 384×256. The computational time of each iterative process using graph cuts is less than 0.15 seconds. Besides the images used in the paper, we also test a large number of real images. For most images, the algorithm converges within eight iterations. Therefore, the total computational time using graph cuts method to deal with an image of size 384×256 is about 1 second, which is much faster than the level set implementation that has been analyzed in many papers [11, 15, 20, 39].

VI. CONCLUSION

A multiple piecewise constant active contour model is presented to generalize the region-based active contour model by Chan and Vese [11]. We further combine the MPC model with the GAC model to get an integrated active contour model that simultaneously exploits both the region feature and edge feature to evolve the curve. We give the level set representation of the proposed model and further show that our model can be effectively optimized by powerful graph cuts algorithms. Experiments show that the proposed model can effectively deal with the images with inhomogeneous object and background and multiple objects with different visual features. The graph cuts implementation greatly improve the computational efficiency.

REFERENCES

[1] A. Blake and M. Isard, Active Contours. Cambridge, MA: Springer, 1998.

[2] N. Paragios and R. Deriche, “Geodesic active contours and level sets for the detection and tracking of moving objects,” IEEE Trans. Pattern Anal. Mach. Intell., vol. 22, no. 3, pp. 226–280, Mar. 2000.

[3] T. Zhang and D. Freedman, “Tracking objects using density matching and shape priors,” in Proc. Int. Conf. Comput. Vis., 2004, pp. 1950–1954.

[4] N. Paragios, Y. Chen, and O. Faugeras, Handbook of Mathematial Models in Computer Vision.. New York: Springer, 2005.

[5] Y. Chen, H. Tagare, S. Thiruvenkadam, F. Huang, D. Wilson, K. Gopinath, R. Briggs, and E. Geiser, “Using prior shapes in geometric active contours in a variational framework,” Int. J. Comput. Vis, vol. 50, pp. 315–328, 2002.

[6] M. Leventon, W. Grimson, and O. Faugeras, “Statistical shape influence in geodesic active contours,” in Proc. IEEE Conf. Computer Vision and Pattern Recognition, 2000, vol. I, pp. 316–323.

[7] V. Caselles, R. Kimmel, and G. Sapiro, “Geodesic active contours,” Int. J. Comput. Vis, vol. 22, pp. 61–79, 1997.

[8] R. Kimmel, A. Amir, and A. Bruckstein, “Finding shortest paths on surfaces using level set propagation,” IEEE Trans. Pattern Anal. Mach. Intell., vol. 17, no. 6, pp. 635–640, Jun. 1995.

[9] M. Kass, A. Witkin, and D. Terzopoulos, “Snakes: active contour models,” Int. J. Comput. Vis, vol. 1, pp. 321–331, 1987.

[10] C. Xu and J. L. Prince, “Snakes, shapes, and gradient vector flow,” IEEE Trans. Image Process., vol. 7, no. 3, pp. 359–369, Mar. 1998.

[11] T. Chan and L. Vese, “Active contours without edges,” IEEE Trans. Image Process., vol. 10, no. 2, pp. 266–277, Feb. 2001.

[12] N. Paragios and R. Deriche, “Geodesic active regions and level set methods for supervised texture segmentation,” Int. J. Comput. Vis., vol. 46, pp. 223–247, 2002.

[13] C. Samson, L. Blanc-Feraud, G. Aubert, and J. Zerubia, “A variational model for image classification and restoration,” IEEE Trans. Patt. Anal. Mach. Intell., vol. 22, no. 5, pp. 460–472, May 2000.

[14] A. Tsai, A. Yezzi, and A. S.Willsky, “Curve evolution implementation of the Mumford–Shah functional for image segmentation, denoising, interpolation, and magnification,” IEEE Trans. Image Process., vol. 10, no. 8, pp. 1169–1186, Aug. 2001.

[15] L. Vese and T. Chan, “A multiphase level set framework for image segmentation using the Mumford and Shah model,” Int. J. Comput. Vis., vol. 50, pp. 271–293, 2002.

[16] D. Mumford and J. Shah, “Boundary detection by minimizing functionals,” in IEEE Computer Society Conference on Computer Vision and Pattern Recognition (CVPR), 1985, pp. 22–26.

[17] Y. Boykov and M. P. Jolly, "Interactive graph cuts for optimal boundary and region segmentation of objects in N-D images", *Proc. International Conference on Computer Vision*, pp. 105-112, 2001.

[18] Y. Boykov and V. Kolmogorov, "An experimental comparison of min-cut/max-flow algorithms for energy minimization in vision", *IEEE Transactions on Pattern Analysis and Machine Intelligence*, vol.26, pp. 1124-1137, 2004.

[19] Y. Boykov and G. Funka-Lea, "Graph cuts and efficient N-D image segmentation", *International Journal of Computer Vision*, vol.70, pp. 109-131, 2006.

[20] S. Lankton and A. Tannenbaum, “Localizing region-based active contours”, *IEEE Transactions on Image Processing*, vol.17, pp. 2029-2039, 2008.

[21] C. Darolti, A. Mertins, C. Bodensteiner, and U.G.Hofmann, “Local region descriptors for active contours evolution”, *IEEE Transactions on Image Processing*, vol.17, pp. 2075-2288, 2008.

[22] D. Mumford and J. Shah, “Optimal approximations by piecewise smooth functions and associated variational problems,” Commun. Pure Appl. Math., vol. 42, pp. 577–685, 1989.

[23] S. Osher and R. Fedkiw, Level Set Methods and Dynamic Implicit Surfaces. New York: Cambridge Univ. Press, 2003.

[24] S. Osher and R. Tsai, “Level set methods and their applications in image science,” Commun. Math. Sci., vol. 1, no. 4, pp. 1–20, 2003.

[25] S. Osher, R. Fedkiw, eds.: Level Set Methods and Dynamic Implicit Surfaces. Springer-Verlag, New York (1998)

[26] Y. Boykov and V. Kolmogorov, “Computing geodesics and minimal surfaces via graph cuts”, in ICCV, 2003.

[27] V. Kolmogorov and R. Zabih, “What energy functions can be minimizedvia graph cuts?”, IEEE Transactions on Pattern Analysis and Machine Intelligence, vol. 26, no. 2, 2004.

[28] D. Fulkerson L. Ford. “Flow in networks”, Princeton University Press, 1962.

[29] D. M. Greig, B. T. Porteous, and A. H. Seheult. Exact maximum a posteriori estimation for binary images. Journal of the Royal Statistical Society, Series B, pages 271–279, 1989.

[30] Y. Li, J. Sun, C. K. Tang and H. Y. Shum, "Lazy snapping", *Proc. SIGGRAPH Conference*, pp. 303-308, 2004.

[31] Y. Boykov, O. Veksler, and R. Zabih, “Fast approximate energy minimization via graph cuts,” IEEE Trans. Pattern Anal. Mach. Intell., vol. 23, no. 11, pp. 1222–1239, Nov. 2001.

[32] A. Chambolle. Total variation minimization and a class of binary mrf models. In Energy Minimization Methods in Computer Vision and Pattern Recognition, pages 136–152. Springer Berlin / Heidelberg, 2005.

[33] Y. Boykov, V. Kolmogorov, D. Cremers, and A. Delong. An integral solution to surface evolution pdes via geo-cuts. ECCV06, pages 409–422, 2006.

[34] J. Darbon and M. Sigelle. Image restoration with discrete constrained total variation part i: Fast and exact optimization. J. Math. Imaging Vis., 26(3):261–276, 2006.

[35] D. Kirsanov and S. Gortler. A discrete global minimization algorithm for continuous variational problems, 2004.

[36] E.A. Dinic, “Algorithm for Solution of a Problem of Maximum Flow in Networks with Power Estimation,” Soviet Math. Dokl., vol. 11, pp. 1277~1280, 1970.

[37] A. V. Goldberg, R. E. Tarjan A new approach to the maximum flow problem. in: Proceedings of the Eighteenth Annual ACM Symposium on Theory of Computing. 1986. 136~146.

[38] C. Rother, V. Kolmogorov and A. Blake, "GrabCut: interactive foreground extraction using iterated graph cuts", *ACM Transactions on Graphics (TOG)*, vol.23, pp. 309-314, 2004.

[39] Egil Bae and Xue-Cheng Tai, Graph Cuts for the Multiphase Mumford-Shah Model Using Piecewise Constant Level Set Methods, June 2008. UCLA, Applied Mathematics, CAM-report-08-36.

[40] X. Bresson, S. Esedoglu, P. Vandergheynst, J.-P. Thiram, S. Osher, Fast Global Minimization of the Active Contour/Snake Model, J. Math. Imaging Vis. 28(7), 151–167 (2007)

[41] Johan Lie, Marius Lysaker and Xue-Cheng Tai, A variant of the level set method and applications to image segmentation. Math. Comp. **75** (2006), no. 255, 1155--1174 (electronic). Also as September 2003. UCLA, Applied Mathematics, CAM-report-03-50.

[42] Johan Lie, Marius Lysaker and Xue-Cheng Tai, A Binary Level Set Model and Some Applications to Mumford-Shah Image Segmentation. IEEE Transection on image processing, vo. 15, no. 5, pp. 1171-1181, 2006.